

## **NUMERICAL AND EXPERIMENTAL INVESTIGATION OF YIELDING FOR COHESIVE DRY POWDER**

**H. Shi, A. Singh, S. Luding and V. Magnanimo**

Faculty of Engineering Technology  
MESA+, University of Twente  
P.O.Box 7500 AE Enschede, The Netherlands

**Abstract** - We study the effect of particle cohesion on the steady state shear strength of a granular material. For cohesive powders, the steady state shear loci (termination loci) from DEM simulations are nonlinear with a peculiar pressure dependence due to the non-linear increase of contact adhesion with pressure in the contact model. Physical experiments are carried out on fine limestone powder in the direct shear box to validate the interesting non-linearity in the material behavior, as detected by the simulations and to provide a basis for calibration of DEM. In order to enhance the reproducibility, the standard test procedure from Jenike shear tester is ameliorated for the direct shear tester. Finally, the difference between the yield (transition from static to flow) and the steady state shear stress (required to maintain shear motion) will be addressed.

### **1. INTRODUCTION**

Granular materials are ubiquitous in our daily life. A special class is powders, which contain fine particles that may flow freely when shaken or tilted. On the other hand, the particles can stick together to form aggregates. Particles smaller than 100  $\mu\text{m}$  are generally found to be cohesive [1]. The likelihood of cohesion increases with decrease in size of the particles. During storage and transportation in powder industry, the material faces various stress conditions, such as compression, abrasion, shearing, etc. The powder which consist of many independent particles may show peculiar flow behavior such as segregation, clustering, shear-band formation, and arching, etc [2].

A topic of particular relevance from the application point of view is to understand the yield behavior of powders, *i.e.*, when they start flowing under shear or what is the shear stress necessary to keep them flowing in order to minimize undesired clustering or piping in different industrial apparatus. In powder technology, yield loci are obtained generally from different shear tests with the most commonly used testers Jenike shear tester [3] and Schulze ring shear tester (RST) [4]. The latter has the advantage compared to Jenike of no shear displacement limit. In soil mechanics, the direct shear box tester is the most commonly used device to obtain yield loci, which was introduced as Casagrande shear box [5] and has been modified by including the possibility of reversed displacement (by reversing shear direction during a test on a single sample) for residual shear strength testing [6].

Recently, simulations are emerging as powerful tool to understand the micro-mechanical behavior of granular materials. The Discrete Element Method (DEM) involves numerical solution of Newton's equations of motion, based on the specification of particle properties and interaction laws [7]. One

goal of the current research in this field is to derive macroscopic continuum behavior for given micro-mechanical properties. Finding a connection between the two scales involves the so-called micro-macro transition [8, 9]. From local averaging over adequate representative volume elements (RVE)s – inside which all particles are assumed to behave similarly – local continuum relations can be obtained [10, 11]. In a previous study, the effect of dry cohesion at contact on the critical state yield stress was addressed in a split bottom Couette cell [11]. The critical-state yield locus shows a peculiar non-linear dependence on the confining pressure based on the non-linear cohesive strength in the contact model [11, 12]. Despite the interesting features, these numerical results have not been validated by experimental results yet.

In this paper, we study the effect of varying confining normal stress on the steady state shear stress (termination locus) as well as the difference between the yield (transition from static to flow) and the steady state shear stress (required to maintain shear motion) for dry cohesive limestone powders. In section 2 the focus is on numerical simulation with methodology and results. The experimental related set-up, reproducibility (proposed modified test procedures) as well as results are presented in section 3, and conclusions with outlooks are given in section 4.

## 2. NUMERICAL SIMULATION

### 2.1 System Geometry

**Split-bottom ring shear cell** The geometry of the system is described in detail in Refs. [2, 13, 14, 15, 16]. It is an assembly of spherical beads confined between two concentric cylinders and a bottom by gravity, with a free top surface. The concentric cylinders rotate relative to each other around the symmetry axis. A ring shaped split at the bottom separates the moving and static bottom parts of the system and the two parts are attached to the outer and inner cylinder respectively. Due to the split, a stable shear band appears at the bottom and it's width considerably increases from bottom to top (see [14] and references therein).

**Material parameters** Due to numerical efficiency, only a quarter of the whole ring system is reproduced. The quarter system is filled with  $N \approx 37000$  spherical particles with density  $\rho = 2000 \text{ kg/m}^3$ . The average size of particles is  $a_0 = 1.1 \text{ mm}$ , with a homogeneous size-distribution of width  $1 - \mathcal{A} = 1 - \langle a \rangle^2 / \langle a^2 \rangle = 0.18922$  (with  $a_{\min}/a_{\max} = 1/2$ ). In order to study the effect of contact cohesion, an adhesive elasto-plastic contact model [10] is used to simulate cohesive particles, involving an elastic limit stiffness  $k_2 = 500 \text{ Nm}^{-1}$ , a plastic stiffness  $k_1 = 100 \text{ Nm}^{-1}$ , and an adhesive "stiffness"  $k_c$ . The simulations were run for different values of the non-dimensional adhesive strength  $Bo$  (a global bond number), as introduced in Ref. [12],  $Bo = f_m / \langle f \rangle = [0, 1.50, 2.85]$  (cohesionless to cohesive), and an artificially small particle friction  $\mu_p = 0.01$  was used to focus on the effect of cohesion. The rolling and torsion friction are inactive. The normal and tangential viscosities are  $\gamma_n = 0.002 \text{ kg s}^{-1}$  and  $\gamma_t / \gamma_n = 1/4$ .

The inertial number, defined as  $I = \dot{\gamma}d \sqrt{\rho/p}$ , where  $\dot{\gamma}$  is the strain rate,  $m$  the mean particle mass, and  $p$  is pressure. Since we are interested in the quasi-static regime, the rotation rate is chosen as  $I \ll 1$  [17]. Our rotation rate,  $f_o = 0.01 \text{ s}^{-1}$  (which corresponds to a contact duration  $t_c = 10^{-5} \text{ s}^{-1}$  for average size of particles  $a_0$ ), satisfies this condition and total simulation time of 50 s is used such that the cylinder completed half a rotation. For the spatial and time averaging, only large times are taken into account, disregarding the transient behavior at the onset of shear.

## 2.2 Method

**Averaging and micro-macro procedure** Translational invariance is assumed in the tangential  $\phi$  direction, and the averaging is performed over toroidal volumes, over many snapshots in time. This leads to fields  $Q(r, z)$  in terms of radial and vertical positions [2, 13]. From simulations, one can calculate the stress tensor as

$$\sigma_{ij} = \frac{1}{V} \sum_{p \in V} m^p (v_i^p)(v_j^p) - \sum_{c \in V} r_i^c f_j^c \quad (1)$$

with particles  $p$ , contacts  $c$ , mass  $m^p$ , velocity fluctuation  $v^p$ , force  $f^c$  and branch vector  $r^c$ . The first term in Eq. (1) is the sum of kinetic energy fluctuations, and the second involves the dyadic product of the contact-force with the contact-branch vector that quantifies the static stress.

For the stress tensor, we can calculate the eigenvalues  $\sigma_1 \geq \sigma_2 \geq \sigma_3$  and define the volumetric part (pressure  $p$ ) as

$$p = \sigma_v = (\sigma_1 + \sigma_2 + \sigma_3)/3 \quad (2)$$

and the deviatoric component as

$$\sigma_{dev} = \sqrt{((\sigma_1 - \sigma_2)^2 + (\sigma_2 - \sigma_3)^2 + (\sigma_3 - \sigma_1)^2)/6} \quad (3)$$

The pressure is the isotropic stress, while  $\sigma_{dev}$  quantifies the normal stress differences like in von-Mises criterion.  $\sigma_{dev}/p$  estimates the effective (macroscopic) friction coefficient of the material.

## 2.3 Results

For a given confining stress (and preparation history), the material can resist shear up to a certain deviatoric (shear) stress, called the "yield stress", beyond which it fails [18]. When yield points  $(p^{(y)}, \sigma_{dev}^{(y)})$  are collected in the  $\sigma_{dev} - p$  plane, a yield locus can be identified, which describes the failure behavior of the material, *i.e.*, its transition from static to dynamic state. When the material is sheared continuously for a long time such that it accumulated large enough shear, it reaches a state which is characterized by the steady state shear stress, *i.e.*, the stress needed to keep the material in motion,  $(p^{(c)}, \sigma_{dev}^{(c)})$ , also referred to as the "critical state" or "termination locus". For simple non-cohesive granular materials, the termination locus can be predicted from a Coulomb type criterion as a straight line with a slope that can be called the (critical) steady state macroscopic friction coefficient  $\mu_{macro} = (\sigma_{dev}^{(c)})/p^{(c)}$ . When adhesion/cohesion is introduced at the contacts, a more complicated picture appears, as described in Ref. [11]. When the material fails, shear strain gets localized in a shear band that, in case of the split-bottom shear cell, is stable, rather wide and stays away from the walls for not too strong cohesion. In order to identify the established steady state shear band, we only consider data with local shear rate above a threshold  $\dot{\gamma}^* = 0.08 \text{ s}^{-1}$  [19]. In Fig. 1, we plot the (shear) deviatoric stress  $\sigma_{dev}$  against pressure  $p$  for different values of Bo. With increasing Bo, the relation between shear stress  $\sigma_{dev}$  and pressure becomes non-linear, as studied in detail in Ref. [11, 12].

## 3. EXPERIMENT

### 3.1 Experimental Setup

**Direct Shear Tester** In this study, we choose the direct shear box as our experimental equipment: the ELE direct shear tester, and its test principle is described in detail in Ref. [20]. The shear box has dimensions as, length  $l$ , width  $w$  being 60 mm and height  $h$  being 30 mm. The horizontal shear velocity  $v$  is set to  $0.002 \text{ m min}^{-1}$  in order to assure the shear deformation is in quasi-static state,

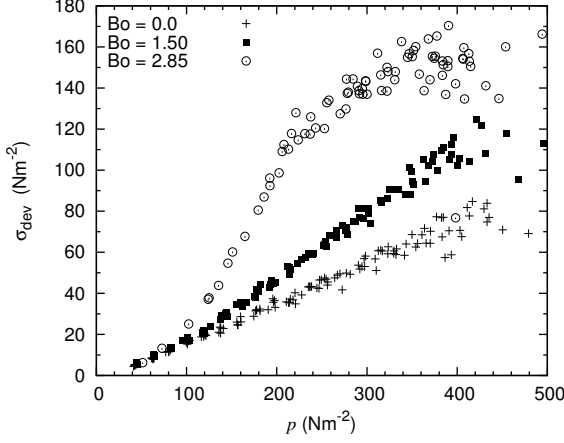


Figure 1: Shear stress  $\sigma_{\text{dev}}$  plotted against pressure  $p$ . Different symbols corresponds to simulations using different particle cohesion parameters  $Bo$ , as given in the inset, and data are given for  $I \approx 0.001$ .

i.e. a global shear rate  $\dot{\gamma}_h = v/h \approx 6 \times 10^{-4} \text{ s}^{-1}$ . However, the local  $\dot{\gamma}$  can be larger due to strain localization. The shear stress  $\tau$  is measured for different confining vertical (normal) stresses  $\sigma_n$  until yield or critical state are reached. The test procedure and specimen preparation are performed by following standard ASTM D3080-98 with modifications, as described in Section 3.2 (see details in Refs. [3, 20]).

**Test Samples** In order to get stable properties and highlight cohesion, dry fine natural calcium carbonate (limestone) powder produced by KSL Staubtechnik GmbH is chosen as test sample: Eskal 500 ( $d_{50} = 4.3 \mu\text{m}$ ,  $\rho_b = 730 \text{ kg/m}^3$ ), where the sample has solid density  $\rho_s = 2700 \text{ kg/m}^3$  and maximum moisture content MC = 0.9 %. The composition of limestone is CaCO<sub>3</sub> (99.1 %), MgO (0.45 %), SiO<sub>2</sub> (0.25 %), Al<sub>2</sub>O<sub>3</sub> (0.10 %), Fe<sub>2</sub>O<sub>3</sub> (0.04 %) and insoluble HCl (0.3 %). The limestone powder is not hygroscopic, not sensitive to humidity and stable in stock. However, it was still carefully brought to laboratory for testing and gain of moisture during transportation was prevented by keeping the samples in plastic bags and plastic box containers if not used. The initial configurations of each sample were kept similar on testing by using the same procedure in order to reduce the influence of changing to fresh samples.

### 3.2 Reproducible Procedures

**Initial Packing Preparation** In order to prepare similar initial packings inside the shear box for different experiments, we use a rotary pluviator to rain the powder until a certain height (10mm) above the shear box is reached. A small scale silo with exact same outlet size to the shear box inlet size is located on the top of the shear box in order to control the pluviation process. This prevents initial clusters of powder by using a spoon or other pouring methods. In analogy with the Jenike shear test, we use an extra rectangular ring on top of the upper part of the shear box to control mass and shape of the initial packing scrap off the excess powder carefully by using a metal blade. The weight of the shear box is then measured to confirm similar sample mass for every test.

**Reproducibility** The core principle to measure the yield locus in powder technology is the step: "Pre-shear", in which the bulk solid samples reach a steady or critical-state (long time shear until steady state), i.e., without any further change in stresses and volume. In this steady state, the sample will lose its memory of preparation history and can be used for further shear tests [18]. However, several proposals can be found in the literature to get a yield locus with Jenike's shear tester (or similar translational shear testers) in only one test: Pitchumani *et al.* modified the conventional multi pre-shear procedure to only one pre-shear and obtained the yield shear stress by step-wisely reducing

normal confining stresses [21]. Tsunakawa and Aoki [22], Ladipo and Puri [23] used the concept of a "constant volume shear test" to measure a yield locus in one single test by moving the lid of the shear box (to keep the sample volume constant). Here we choose the same procedure as conventional Jenike and Schulze shear tests and apply it to the geo-mechanical direct shear tester.

For the termination locus (critical or steady state yield locus), in order to reduce the sample numbers and therefore reduce the deviation between fresh samples, we propose a step-wise increase in normal confining stress during each steady shear test and reuse the same sample by returning it back to the initial state (horizontal displacement of shear box  $\delta = 0$ ). The influence of reversing the shear direction on the shear behavior is small and the independence of residual strength (steady state shear stress) on stress history (*i.e.* previous shear) has been proved by Suzuki *et al.* [6].

#### **Procedure of Yield Locus Test** Analogous to Jenike and Schulze shear tests:

- a) Place the metal lid onto the shear box.
- b) Carefully place the shear box into the direct shear device and rotate the horizontal screws to keep it fixed in the horizontal direction.
- c) Remove two alignment screws from the shear box and place them in the screw holes of the bottom box.
- d) Place the loading hanger onto the lid and make sure that the hanger is free to move in horizontal direction.
- e) Initialize the three gauges (Horizontal displacement gage, vertical displacement gage and shear load gage) to zero.
- f) Set the vertical load (pre-shear stage) to a pre-determined value by adding a certain weight onto the loading hanger.
- g) Start the test with pre-selected velocity so that the rate of shearing is constant, and horizontal displacement, vertical displacement and shear force can be recorded.
- h) Stop shearing when the system reaches a steady state, characterized by a constant shear force; then remove the vertical load and reverse the shear box until the shear force becomes zero.
- i) Place a vertical load (shear stage) which is smaller than the pre-shear load and start shearing again until the horizontal shear force reaches a peak value or the horizontal displacement reaches 15 mm.
- j) Record the peak value of the horizontal force, the vertical load and the vertical displacement, then reverse the shear box until its initial position ( $\delta = 0$ ) and repeat step a) to i), but change the vertical load to another level in step i).

#### **Procedure of Termination Locus Test** As described above, the termination locus is tested by increasing normal load in steps as:

1. Place the wood lid (first very small vertical load) onto the shear box and follow steps b) and c), as mentioned in the Yield Locus Test.
2. Place the loading hanger aside and make sure the hanger is not touching moving parts of the shear device.
3. Initialize the three gauges (Horizontal displacement gage, vertical displacement gage and shear load gage) to zero.

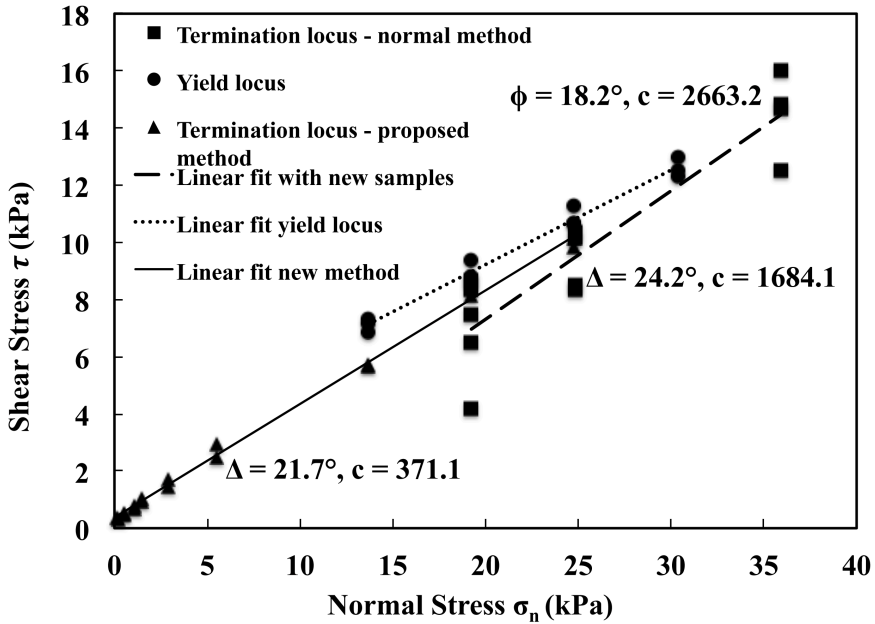


Figure 2: Yield locus, termination locus from normal method and proposed method i.e. Yield/critical shear stress  $\tau$  plotted against normal confining stress  $\sigma_n$ . The material used is Eskal 500 with  $d_{50} = 4.3 \mu\text{m}$  and  $\rho_s = 2700 \text{ kg/m}^3$ , shear rates  $v_s = 2 \text{ mm/min}$  ( $\dot{\gamma}_h \approx 6 \times 10^{-4} \text{ s}^{-1}$ ).

4. Start the test with pre-selected velocity so that the shear rate is constant, and the horizontal displacement, vertical displacement and shear force can be recorded.
5. Stop the shearing when shear force is no longer increasing (reaching steady state) or the horizontal displacement reaches 15 mm, record the vertical load and maximum shear force and then reverse the shear box until its initial position ( $\delta = 0$ ) is reached.
6. Increase the vertical load to 0.1 kg (0.27 kPa), 0.2 kg (0.54 kPa), 0.4 kg (1.09 kPa), 0.8 kg (2.18 kPa), 1.6 kg (4.36 kPa), 3.2 kg (8.72 kPa) respectively and repeat step 3) to 5).
7. Place the metal lid and loading hanger onto metal lid (which is 5 kg vertical load or 13.6 kPa) and repeat step 3) to 5).
8. Increase the normal load by adding a certain weight on hanger: 2.04 kg (5.56 kPa), 4.08 kg (11.1 kPa), 6.12 kg (16.7 kPa), 8.16 kg (22.2 kPa) and repeat step 3) to 5), or stop the test when the metal lid is under the surface of the upper shear box after adding a weight.

### 3.3 Results

The experiments are carried out with limestone powder as mentioned above and results for Eskal 500 are shown in Fig. 2. We plot the shear stress  $\tau$  against normal confining stress  $\sigma_n$  to show the differences between the yield locus and the termination locus from both normal and proposed methods. The yield locus is obtained by using  $\sigma_n = 35.9 \text{ kPa}$  in the pre-shear stage followed by shear at 13.7, 19.2, 24.8 and 30.4 kPa stress levels and the tests are repeated three times for similar virgin samples in order to get representative results. The angle of internal friction and the corresponding pre-confined cohesion are found to be  $\Phi \approx 18.2^\circ$  and  $c \approx 2.66 \text{ kPa}$ , respectively. In order to get the termination locus, first we use the conventional method as Jenike, *i.e.*, three stresses (19.2, 24.8, and 35.9 kPa) are chosen as normal confining stress  $\sigma_n$  (each stress level is tested with four virgin sample). The stationary angle of internal friction is  $\Delta \approx 24.2^\circ$  and the corresponding cohesion  $c \approx 1.68 \text{ kPa}$ . We also test another two samples following the proposed new reversed procedure for different normal stresses: 0.24, 0.55, 1.09, 1.43, 2.87, 5.48, 13.7, 19.2 and 24.8 kPa, and the stationary angle of internal

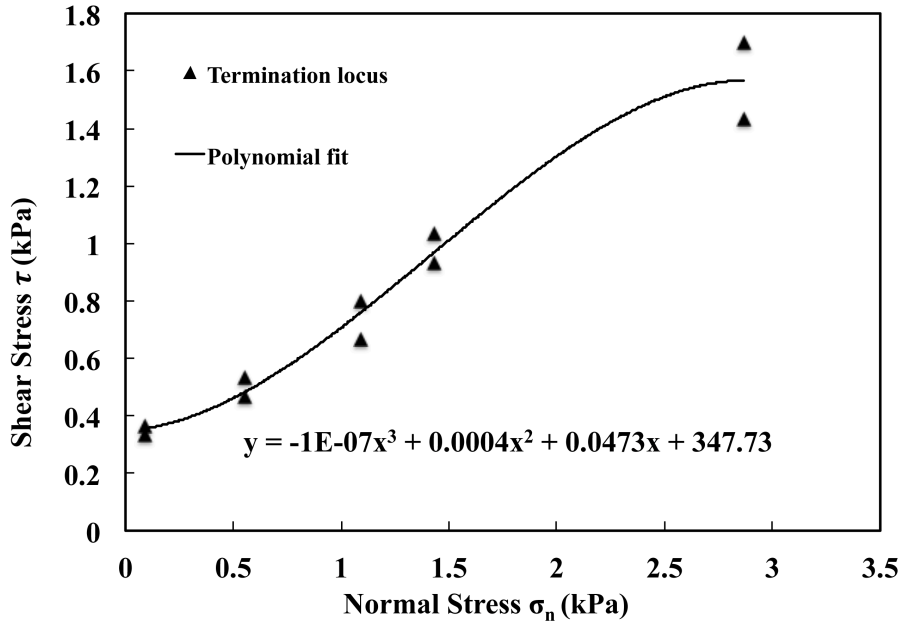


Figure 3: Termination locus, Critical state shear stress  $\tau$  plotted against normal confining stress  $\sigma_n$  under low normal confining stresses ( $\sigma_n \leq 2.87$  kPa).

friction and the corresponding cohesion are found to be  $\Delta \approx 21.7^\circ$  and  $c \approx 0.37$  kPa respectively. Compared to the result from the conventional method, data obtained by using the new method show much less fluctuations between virgin samples, which gives us a possibility to investigate the cohesive powder behavior under low confining stress conditions. The termination locus is linearly well fitted for normal stresses above 2.87 kPa, while for stresses below 2.87 kPa, a non-linearity appears, as shown in Fig. 3, which qualitatively reflects the behavior in Fig. 1. The low-pressure behavior can be described by a 3rd order polynomial. However, more results from different particle sizes have to be added to get more evidence on this non-linearity introduced by cohesion.

#### 4. CONCLUSION

The effect of micro-mechanical parameters on the macroscopic rheological properties of a granular material have been studied by means of the discrete element method (DEM). Different features have been highlighted by varying contact cohesion. Different loci are studied experimentally for dry limestone powder, and the non-linearity of low confining stress region is highlighted. Qualitative agreement has been achieved by comparing simulations and experiments but more tests are necessary to confirm its significance and reliability. The termination locus (critical state shear stress) is found to be a linear function of pressure, as predicted by the Mohr-Coulomb criterion [24], in non-cohesive materials. Under low normal confining stress (loose packing with low bulk density), cohesion appears to dominantly influence the shear behavior. Further verification with different particle sizes (different cohesion) and comparison between shear testers (Schulze ring shear tester and Direct shear tester) is in processing and will be addressed future study.

#### 5. ACKNOWLEDGMENT

Financial support through the “T-MAPPP” project of the European-Union-Funded Marie Curie Initial Training Network FP7 (ITN607453) is acknowledged. See <http://www.t-mappp.eu/> for more information.

## 6. REFERENCES

- [1] J. Bridgwater. Fundamental powder mixing mechanisms. *Powder Technol.*, 15:215, 1976.
- [2] S. Luding. The effect of friction on wide shear bands. *Particulate Science and Technology*, 26(1):33–42, 2007.
- [3] A. W. Jenike. Storage and flow of solids, bulletin no. 123. *Bulletin of the University of Utah*, 53(26):198, 1964.
- [4] D. Schulze. Development and application of a novel ring shear tester. *Aufbereitungstechnik*, 35:524–535, 1994.
- [5] J. Schwedes. Vergleichende Betrachtungen zum Einsatz von Schergeräten zur Messung von Schüttguteigenschaften. *Proc. PARTEC, Nürnberg*, pages 278–300, 1979.
- [6] M. Suzuki, S. Tsuzuki, and T. Yamamoto. Residual strength characteristics of naturally and artificially cemented clays in reversal direct box shear test. *Soils and foundations*, 47(6):1029–1044, 2007.
- [7] M. P. Allen and D. J. Tildesley. *Computer Simulation of Liquids*. Oxford University Press, Oxford, 1987.
- [8] P. A. Vermeer, S. Diebels, W. Ehlers, H. J. Herrmann, S. Luding, and E. Ramm, editors. *Continuous and Discontinuous Modelling of Cohesive Frictional Materials*, Berlin, 2001. Springer. Lect. Not. Phys. 568.
- [9] M. Lätsel, S. Luding, and H. J. Herrmann. Macroscopic material properties from quasi-static, microscopic simulations of a two-dimensional shear-cell. *Gran. Matt.*, 2(3):123–135, 2000.
- [10] S. Luding. Cohesive frictional powders: Contact models for tension. *Gran. Matt.*, 10:235–246, 2008.
- [11] S. Luding and F. Alonso-Marroquín. The critical-state yield stress (termination locus) of adhesive powders from a single numerical experiment. *Gran. Matt.*, 13:109–119, 2011.
- [12] A. Singh, V. Magnanimo, K. Saitoh, and S. Luding. Effect of cohesion on shear banding in quasi-static granular material. *Phys. Rev. E*, 90(022202), 2014.
- [13] S. Luding. Constitutive relations for the shear band evolution in granular matter under large strain. *Particuology*, 6(6):501–505, 2008.
- [14] J. A. Dijksman and M. van Hecke. Granular flows in split-bottom geometries. *Soft Matter*, 6:2901–2907, 2010.
- [15] D. Fenistein, J. W. van de Meent, and M. van Hecke. Universal and wide shear zones in granular bulk flow. *Phys. Rev. Lett.*, 92:094301, 2004.
- [16] D. Fenistein and M. van Hecke. Kinematics – wide shear zones in granular bulk flow. *Nature*, 425(6955):256, 2003.
- [17] F. da Cruz, S. Emam, M. Prochnow, J. J. Roux, and F. Chevoir. Rheophysics of dense granular materials : Discrete simulation of plane shear flows. *Phys. Rev. E*, 72:021309, Aug 2005.
- [18] J. Schwedes. Review on testers for measuring flow properties of bulk solids. *Granular Matter*, 5(1):1–45, 2003.

- [19] A. Singh, V. Magnanimo, K. Saitoh, and S. Luding. Role of gravity or confining pressure and contact stiffness in granular rheology. *arXiv preprint arXiv:1412.0874*, 2014.
- [20] D. Schulze. Powders and bulk solids. behaviour, characterization, storage and flow. *Springer*, 2008.
- [21] B. Pitchumani, A. K. Sharma, and G. G. Enstad. A simplified procedure for flow property testing using the jenike shear tester. In *5th International Conference on Bulk Materials Storage, Handling and Transportation: Proceedings*, page 371. Institution of Engineers, Australia, 1995.
- [22] H. Tsunakawa and R. Aoki. Measurements of the failure properties of granular materials and cohesive powders. *Powder Technology*, 33(2):249–256, 1982.
- [23] D.D. Ladipo and V.M. Puri. Computer controlled shear cell for measurement of flow properties of particulate materials. *Powder technology*, 92(2):135–146, 1997.
- [24] C.O. Mohr. Welche Umstände bedingen die Elastizitätsgrenze und den Bruch eines Materials. *Zeitschrift des Vereins Deutscher Ingenieure*, 46(1524-1530):1572–1577, 1900.